Q. J. R. Meteorol. Soc. **00**: 1–14 (0000)
Published online in Wiley InterScience
(www.interscience.wiley.com) DOI: 10.1002/qj.000

Global satellite measurements of HDO and implications for understanding the transport of water vapour into the stratosphere

V. H. PAYNE[1]* D. NOONE[2], A. DUDHIA[3], C. PICCOLO[3], AND R. G. GRAINGER[3]

[1]*Was at University of Oxford, UK, now at Atmospheric and Environmental Research, Inc, USA*
[2]*University of Colorado at Boulder, USA*
[3]*University of Oxford, UK*

Abstract: The deuterium content of water vapour in a given air mass is sensitive to its temperature and condensation history. Isotopic measurements therefore have the potential to shed light on the transport of air and water vapour into the stratosphere. Previous measurements of the isotopic composition in the upper troposphere and stratosphere have been sparse in terms of both spatial and temporal coverage. Presented here are retrievals of the deuterium content of water vapour (HDO, or δD) from the MIPAS satellite instrument. These retrievals offer the first global scale coverage of the isotopic composition of water vapour in this altitude region and span a time period of almost two years. The spatial coverage and the time span of the dataset offer previously unattainable insight into the mean seasonal and spatial distributions of the isotopic composition of water vapour in the upper troposphere and stratosphere. Measurements of HDO are extremely challenging due to low sensitivity in the spectra at low temperatures and water vapor amounts. Nonetheless, the data show a number of interesting results.

Zonal mean profiles show the greatest depletion in δD in the tropical upper troposphere, with decreasing depletion with altitude in the stratosphere due to the influence of methane oxidation. Seasonal zonal means also show a strong depletion in the southern polar spring at around 300 mbar, which is thought to be related to the occurrence of polar stratospheric clouds and dehydration events in the polar vortex.

Geographically, the regions and time periods where the greatest depletions are observed in the tropical upper troposphere are those associated with strong convective activity. Results confirm that temporal variability is central to the transport of water vapour into the TTL and stratosphere. The data presented here shows an annual cycle in δD in the tropical tropopause layer (TTL) which is tied to temperature and suggests that this signature propagates upwards into the stratosphere. The data also shows a number of points where extremely dry air is associated with relatively enriched δD values. We postulate that these points are evidence of ice lofting.

KEY WORDS convection, horizontal transport, isotopic composition, MIPAS, ozone, stratosphere–troposphere exchange, tropical tropopause layer

Received 14th August 2006; Revised 2nd May 2007; Accepted 24th May 2007

1 Introduction

1.1 Water vapour in the upper troposphere and stratosphere

It is widely acknowledged that the amount of water vapour in the lower stratosphere is changing (Rosenlof 2001). Changes in stratospheric water vapour may impact upon tropospheric warming, stratospheric cooling (Forster and Shine 1999) and on the availability of radicals which affect ozone destruction (Kirk–Davidoff *et al.* 1999). An understanding of these changes is therefore of paramount importance in the prediction of future climate and ozone recovery, but the reasons for the observed changes are not well understood.

Increases in stratospheric water vapour can be partly accounted for by increases in methane — the oxidation of which is a signifi cant source of stratospheric water vapour. However, the observed trends in water vapour cannot be accounted for by methane alone (WMO 2000). The observed increases may be influenced by changes in the details of the mechanisms controlling the transport of water vapour into the stratosphere (Rosenlof 2003) from the troposphere. These mechanisms are currently not well understood, because the range of possible active processes is large. Since measurements of the isotopic composition of water vapour provide additional constraints on the water budgets, they offer potential insight into these mechanisms and therefore potential for a better understanding of changes in stratospheric water vapour.

The work presented here has involved development of a new satellite–based climatology of HDO in the upper troposphere and stratosphere. The Michelson Interferometer for Passive Atmospheric Sounding (MIPAS) instrument on Envisat measures high resolution infrared spectra from which HDO and H_2O concentrations can be retrieved from cloud–free scenes. The retrieved estimates are used to create an HDO climatology derived from two

* Correspondence to: Vivienne H. Payne, Atmospheric and Environmental Research, Inc (AER), 131 Hartwell Avenue, Lexington, MA 02421, USA. E-mail: vpayne@aer.com

years (2002-2004) of global measurements. This provides an unprecedented view of the isotopic composition of water vapour in the upper troposphere and stratosphere.

1.2 Transport of water vapour into the stratosphere

Most of the transport of tropospheric air into the stratosphere takes place in the tropics. Brewer (1949) envisioned the flux into the stratosphere as a slow, large–scale upwelling through the tropical tropopause (located at around 100 mbar). In this model, it is assumed that the tropopause region acts as a "cold trap", where air passing through is dehydrated to the region's local minimum saturation mixing ratio. Observations of thin cirrus near the tropopause (e.g. Winker and Trepte 1998) suggest the existence of frequent uplift near the tropopause. The fact that sub–visible cirrus and supersaturated air are frequently observed in the region of the tropical tropopause, suggest that steady uplift may be a viable mechanism. However, it has also been argued that the absence of a thick cirrus deck throughout the tropopause argues against uniform, steady uplift (Robinson 1980). Also, this model is not consistent with observations that tropopause temperatures show a long–term cooling trend (Rosenlof 2003) during the time that the water vapour in the lower stratosphere was increasing.

A possible mechanism that overcomes these problems is *in situ* dehydration over meso– or synoptic–scale convective systems, or in the crests of slow–moving propagating waves. These systems and waves can lift the lower stratosphere, producing substantial cooling in some cases (e.g. Fritsch and Brown 1982; Potter and Holton 1995). If the lifting persists for a sufficient duration, there can be time to condense and remove significant amounts of water vapour. Although the behaviour of these systems is transient, the effects are large enough to affect the mean water vapour distribution over time. An alternative theory is that energetic convection originating near the surface overshoots the tropopause and mixes with stratospheric air, thereby transferring mass from the troposphere directly into the stratosphere (Danielson 1982).

Sherwood and Dessler (2000) suggest a "mixing layer hypothesis", involving the "tropical tropopause layer" (TTL). The TTL can be thought of as a reasonably shallow layer of the atmosphere where air that is distinctly tropospheric and air that is distinctly stratospheric mix. Within the TTL the distinction between the two air masses is less clear. In this hypothesis, air is dehydrated rapidly as suggested by Danielson (1982) but convective detrainment occurs at variable levels throughout the depth of the TTL. The bottom of the TTL is close to the level of neutral buoyancy (LNB) for convective plumes. Air detraining near the bottom of the TTL need not have overshot and will be relatively moist compared to the stratospheric mean. Air detraining at higher altitudes must have originated in more energetic and warmer updrafts and/or overshot significantly. This "young" air has been dehydrated by mixing with stratospheric air at the maximum altitude of the overshoot. The younger, dehydrated air spreads horizontally from the convective region, where it mixes with "older", moister air that detrained earlier at lower altitudes and has slowly risen to this altitude. Air on any given potential temperature surface will therefore have a spectrum of ages, because the timescale of isentropic mixing is longer than that of energetic convective events. At locations further from intense convection, this spectrum will be weighted more toward older air as the layer tends towards homogeneity. It is important to consider horizontal, as well as vertical, motion. Air may also be dehydrated as it moves horizontally through a cold pool region (Holton and Gettelman 2001).

An understanding of the relative contributions of large–scale slow ascent, rapid overshooting convection and horizontal transport to the composition of TTL air will be necessary to anticipate how changes in various controlling factors (convection intensity, detrainment altitude, cloud microphysics, temperature) may alter the water vapour content of air entering the stratosphere in the future.

1.3 The isotopic composition of water vapour

The isotopic composition of water vapour in the upper troposphere and stratosphere is sensitive to the temperature, precipitation and chemical history of the air and therefore provides an additional observational constraint for determining the relative importance of the possible transport mechanisms.

Isotopic compositions are reported in delta notation, where the deuterium content of a sample, δD, is defined in equation 1.

$$\delta\mathrm{D} = \left(\frac{\mathrm{R_{sample}}}{\mathrm{R_{std}}} - 1 \right) \times 1000 \qquad (1)$$

For water, $\mathrm{R_{sample}}$ is the D/H mole ratio in a water sample and $\mathrm{R_{std}}$ is the D/H ratio for the international reference material Vienna Standard Mean Ocean Water (VSMOW) ($\mathrm{R_{std}} = 1.55 \times 10^{-4}$). Thus the delta value, δD–H_2O, represents the deviation of the D/H ratio of a water sample from that of the VSMOW standard, expressed in "per mil" (‰).

The isotopic composition of water vapour in the troposphere is largely determined by phase changes. When water evaporates from the oceans, the lighter isotopologues evaporate preferentially over the heavier isotopologues (the "vapour pressure isotope effect"). Water vapour in the lower troposphere is therefore depleted in deuterium relative to ocean water. Large–scale ascent, turbulence and convective events may cause

DOI: 10.1002/qj

this lower tropospheric air to rise. Vapour condenses into cloud droplets and ice particles, leaving upper tropospheric water vapour further depleted in deuterium relative to VSMOW.

The isotopic composition of water vapour at a given time and location is dependent on the temperature and condensation history of the pathway by which the location was reached. Air which has ascended slowly, with condensation occurring along the way, should show strong isotopic depletion because of the vapour pressure effect. If the only change in vapour were due to condensation removed during ascent, a Rayleigh distillation curve could be used to explain the bulk features of the change in δD relative to changes in H_2O concentration. Given typical humidities and condensation temperatures, a Rayleigh model gives upper tropospheric δD values of around -900 ‰. Observed values in the range -870 to -460 ‰ (e.g. Webster and Heymsfield 2003) do not show such extreme depletion. Smith (1992) suggested that the reason that the observed depletions are less pronounced than a Rayleigh prediction is that convective events may lead to lofting of ice particles from the mid–troposphere (where the prevailing deuterium content of water vapour is higher than in the upper troposphere) and that these ice particles then sublimate into the vapour phase, leading to less depletion in air associated with rapid convection. Satellite observations of large ice particles near the tropopause in convectively active regions have recently been obtained using the Microwave Limb Sounder (MLS) on NASA's Aura satellite (Wu *et al.,* 2006), although the importance of this ice lofting on the upper tropospheric humidity budget has not yet been determined.

The upper tropospheric values obtained from a Rayleigh model do of course depend on the initial temperature and δD. A starting point over ocean, with δD close to zero, would give different results than a starting point over land, where δD is likely to be further from zero due to rainout of heavy isotopes and/or other condensation/evaporation processes (Smith 1992). In addition, the Rayleigh distillation model assumes that isotopic fractionation occurs through equillibrium processes. Isotopic fractionation in water vapour may also occur through non-equilibrium processes, for example in the presence of supercooled water. Supersaturated conditions result in greater effects from non-equilibrium processes. The presence, or otherwise, of condensation nuclei would be expected to play a role here. Non-equilibrium effects are much weaker in D/H ratios than in, say, $^{18}O/^{16}O$ ratios (Dansgaard 1964), but the extent to which these effects affect the analysis of the data presented in this paper is not known. Horizontal transport in the TTL may further complicate the analysis, since in a given air parcel, water may freeze out, but ice crystals from above may also fall and re-evaporate. It takes on the order of a week for air to circle the tropics, so freezing and re-evaporation could occur multiple times for a given air parcel before the air enters the stratosphere.

In the stratosphere, water vapour is produced by the oxidation of methane and, to a lesser extent, molecular hydrogen. Both CH_4 and H_2 are enriched in deuterium relative to VSMOW (McCarthy *et al.* 2004) and so the deuterium depletion shows a reduction with increasing altitude in the stratosphere. As such, we expect to find maximum depletion in the region of the tropical tropopause, where the depleting effects of condensation are at their most extreme, with less depletion as one moves upwards and chemical sources dominate over condensation processes.

Although the atmospheric hydrology is an intricate balance of numerous contributing processes, it is clear that different mechanisms of atmospheric water vapour transport will lead to different isotopic signatures in the water vapour in the upper troposphere and lower stratosphere. As such, isotopic measurements allow some aspects of the dominating processes to be evaluated.

1.4 Other measurements

In situ measurements of the isotopic composition of water vapour in the upper troposphere and lower stratosphere from aircraft platforms are challenging because of the low absolute concentration of both H_2O and HDO at low temperatures. The low concentrations prohibit the collection of vapour samples for analysis with traditional isotope mass spectrometers, as can be done in the lower troposphere (e.g. Taylor 1972; Enhalt 1974). In recent years there has been increasing success using laser spectroscopy (e.g. Webster and Heymsfield 2003). These *in situ* measurements have the advantage of high accuracy and of high spatial and temporal resolution, providing the opportunity to resolve small–scale processes. Remote sounding measurements from aircraft and balloon platforms have also been made, yielding profile information on the isotopic composition of water vapour (e.g. Johnson *et al.* 2001a; Dinelli *et al.* 1991; Coffey *et al.,* 2006). The long-term dataset of interferometric aircraft-based measurements analysed by Coffey *et al.* (2006) show a trend in δD in the lower stratopsheric column water vapour, with depletion increasing by 5-6 ‰ per year over a 27 year period.

Space–based observations of HDO in the upper troposphere and stratosphere in cloud–free conditions have been made from the Atmospheric Trace Molecule Spectroscopy (ATMOS) experiment (Moyer *et al.* 1996; Kuang *et al.* 2003). These observations were limited in spatial and temporal coverage due to the short duration of the Space Shuttle mission on which the instrument was used. Observations of HDO in the stratosphere have also been made from the Odin Sub–millimeter Radiometer (Nordh *et al.* 2003; Urban *et al.* 2004), but the sensitivity of these measurements extends down no further than

DOI: 10.1002/qj

around 20 km and so they do not capture the important tropopause region. HDO measurements in the upper troposphere and lower stratosphere are also possible from the Atmospheric Chemistry Experiment (ACE) (Boone *et al.*, 2005), although this solar occultation instrument requires long time periods to build up good coverage in the tropics. Tropospheric measurements of HDO, complimentary to an analysis of the upper troposphere, have been made by the Tropospheric Emission Spectrometer (TES) on the Aura satellite (Worden *et al.* 2006; Worden *et al.* 2007).

Studies based on previous measurements have tended to focus on the "entry value" (Moyer *et al.* 1996; Johnson *et al.* 2001a; McCarthy *et al.* 2004) of δD — the value of δD for water vapour entering the stratosphere in the tropics. Values quoted are in the range of -650 to -670 ‰. It should be pointed out that this "entry value" is not the same as the maximum depletion, which is expected (e.g. from models [Schmidt *et al.* 2005]) to have a more strongly negative value and be located at a lower altitude than the presumed "entry point". It should also be pointed out that aircraft measurements (Webster and Heymsfield 2003) in the upper troposphere and lower stratosphere have shown a wide range of values of δD in this region. As such, it remains unclear whether a single value is the most useful quantity to consider. Furthermore, previous measurements of HDO in the upper troposphere and stratosphere have been isolated in space and time, not yielding enough data to enable climatological distributions to be established. It is not clear how representative they are of mean conditions.

Here we present measurements from the Michelson Interferometer for Passive Atmospheric Sounding (MIPAS), a satellite–borne limb–sounding instrument. MIPAS offers the advantage of unprecedented spatial and temporal coverage in this region. Section 2 describes the MIPAS instrument. HDO is not one of the core MIPAS species [which are processed operationally by the European Space Agency (ESA)] and so a separate retrieval approach has been adopted. The retrieval approach is also described in Section 2. The results obtained are presented and discussed in Section 3.

2 MIPAS measurement of HDO

2.1 The MIPAS satellite instrument

MIPAS is one of the core experiments on the ESA Envisat satellite, launched in March 2002. MIPAS data used here is from the period spanning July 2002 until March 2004. During this period, MIPAS measured infrared atmospheric limb emission spectra in the range 685–2410 cm^{-1} (wavelengths of 14.5–4.1 μm) sampled at 0.025 cm^{-1} over an altitude range 6–68 km. (Spectra measured after March 2004 are sampled at a lower spectral resolution.) After suitable ground processing, these spectra allow retrieval of profiles of atmospheric temperature, pressure and numerous trace gases. The MIPAS data offers near–continuous global coverage, both day and night, during this time period. The MIPAS instrument field of view (FOV) spans 3 km in the vertical, while the distance between adjacent limb scans is around 500 km. Further technical details of the MIPAS instrument are described by Fischer and Oelhaf (1996) and ESA (2002), while details of the operational processing can be found in Ridolfi *et al.* (2000).

As an infrared limb emission spectrometer, measurements from MIPAS are sensitive to clouds. A cloud in the line of sight leads to high background continuum in the spectra, making it difficult to discern trace gas emission lines and therefore to retrieve trace gas concentrations. For this reason, cloud–contaminated spectra have been excluded from the results shown here. This sampling limitation should be borne in mind when interpreting final results. The method of cloud detection used relies on the ratio of the radiance in two small regions of the spectrum (Spang *et al.* 2004). In the data used here, there were practically no measurements flagged as "cloud–free" at the 6 km nominal tangent altitude in the tropics. At the 9 km nominal altitude, 9% of tropical limb scans were deemed cloud–free, rising to 21% at 12 km, 47% at 15 km and 89% at 18 km. No tropical measurements above 21 km were flagged as cloudy.

2.2 Retrieval method

Retrievals of HDO from MIPAS spectra have been performed using the MIPAS Orbital Retrieval using Sequential Estimation (MORSE), a retrieval code developed at the University of Oxford (Dudhia 2005). The main difference between MORSE and the ESA operational retrieval is that, whereas the ESA retrieval is a least–squares fit, MORSE uses an optimal estimation method (Rodgers 2000) with *a priori* constraints, which is more robust for low signal to noise.

Microwindows were selected using an algorithm developed at the University of Oxford (Dudhia *et al.* 2002a), which models the propagation of both random and systematic errors through the retrieval. The microwindows used in the HDO retrievals are shown in Table 2.2, while the error analysis is discussed in more detail in the following section. Look–up tables (for absorption coefficients) and irregular spectral grids (Dudhia *et al.* 2002b) were calculated for the microwindows detailed in Table 2.2. Retrievals were then performed in series in the following sequence: joint retrieval of pressure, temperature and H_2O, retrievals of potential interfering species (O_3, HNO_3, CH_4 and N_2O) and a joint retrieval of HDO and H_2O. The intention behind the joint retrievals is to minimise the contribution from systematic errors (Worden *et al.* 2006). The joint pressure/temperature/H_2O retrieval and the interfering species retrievals were performed

DOI: 10.1002/qj

using the microwindows used for the ESA operational retrievals (Carli *et al.* 2004). The joint HDO/H_2O retrieval was performed using the newly-selected microwindows in Table 2.2. Further details on the retrieval approach for HDO can be found in Payne (2005). Note that the H_2O is retrieved twice. The reason for this is that although it is desirable to perform a joint HDO/H_2O retrieval, the microwindows selected to contain the best information on HDO may not be the best microwindows for H_2O. A joint HDO/H_2O retrieval using strong H_2O lines could result in the H_2O dominating the retrieval fit at the expense of the HDO part of the retrieval. For this reason, it was decided to retrieve H_2O first using microwindows where the H_2O had a strong signal, and then to use this information to constrain the joint H_2O/HDO retrieval, performed with the microwindows in Table 2.2.

2.3 Error analysis

Systematic errors considered in the microwindow selection process include forward model parameter errors, such as uncertainties in the concentrations of other trace gases and in spectroscopic parameters, as well as instrumental effects such as uncertainties in the radiometric gain, spectral calibration and instrument line shape. Systematic errors, unlike errors due to random noise, are correlated between spectral points and between different tangent altitudes.

Error analyses from the HDO and H_2O microwindows were used to construct an estimate of the total error on a δD profile. The results are shown in Figure 1. The random error can be reduced by averaging profiles, but the total systematic error estimate could be taken as a limit on the accuracy of the δ–values that can be obtained using these microwindows and this approach to the retrievals. However, this would be an overly conservative estimate of the limit since systematic error contributions due to temperature, pressure and contaminant gases might be expected to become decorrelated over the timescale of a few days, and might therefore also be reduced by averaging. Based on this analysis, the accuracy on a single profile of δD is 80 ‰, while the accuracy on an average of a large number of profiles is 20 ‰. Note that the impact of many systematic errors, such as temperature and gain, are reduced when considering the ratio of HDO to H_2O, rather than the absolute concentration of HDO.

The averaging kernel matrix $\mathbf{A}$ (Rodgers 2000) is a useful indicator of retrieval quality. $\mathbf{A}$ is defined as

$$\mathbf{A} = \mathbf{I} - \mathbf{S}_a^{-1}\mathbf{S}_x, \qquad (2)$$

where $\mathbf{I}$ is the identity matrix, $\mathbf{S}_a$ is the *a priori* covariance matrix and $\mathbf{S}_x$ is the retrieval covariance matrix. Figure 2 shows the rows of a representative averaging kernel from a single profile retrieval of HDO. The width of the averaging kernels is a measure of vertical resolution, while the sum of each row of the matrix gives an indication of how

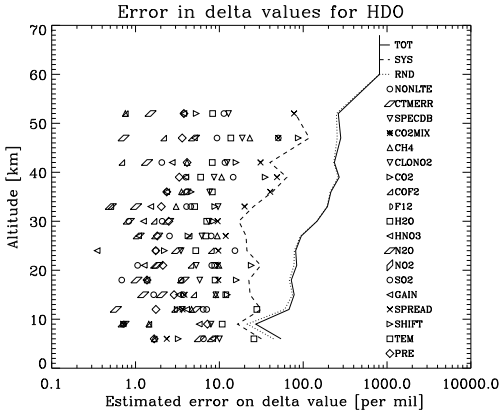

Figure 1. Estimated error components on δD for a single–profile retrieval, showing contributions from noise (RND) as well as from systematic (SYS) sources. Systematic error sources considered (shown by symbols) include contributions due to temperature, pressure and contaminant gases as well as instrumental effects and certain assumptions made in the forward model (Dudhia *et al.* 2002). The instrumental effects considered are the radiometric gain (GAIN), the spectral shift (SHIFT) and uncertainties in the instrument line shape (SPREAD). Forward model errors considered include the assumption of local thermal equilibrium (NLTE), errors in the continuum (CTM) and uncertainties in the spectroscopic parameters (SPECDB). Temperature errors dominate the systematic error budget at the lowest altitudes. At higher altitudes, the dominant systematic errors are the uncertainties in the spectral shift and the instrument line shape.

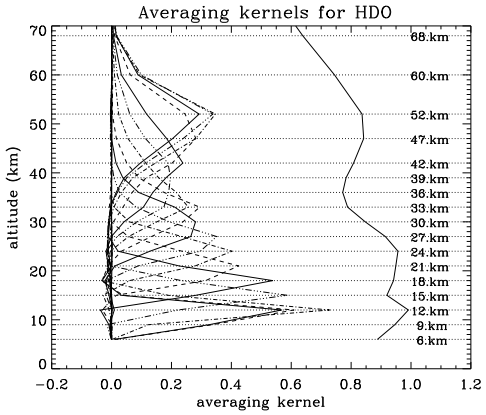

Figure 2. Averaging kernels for a single–profile HDO retrieval. The width of each curve suggests vertical resolution ranging from around 5 km at the lowest tangent altitudes to around 15 km at a tangent altitude of 52 km. The solid line on the right of this plot shows the sum of the row of the averaging kernel at each nominal altitude. Between 6 and 30 km, this quantity is close to 1.0, indicating that the information in the retrieved profile comes from the measurement rather than from the *a priori* constraint used in the retrieval.

sensitive the retrieval is to the true profile. Where the sum of the row is approximately equal to 1, the information comes from the measurement rather than from the *a priori* constraint. From the averaging kernels shown in Figure 2, useful retrievals of HDO are obtained between 6 and 30 km. The averaging kernels do vary from scan to scan, so the useful retrieval altitude range also varies somewhat.

DOI: 10.1002/qj

Table I. Spectral and altitude ranges of the microwindows used/selected for the retrievals

Isotope	Microwindow label	Spectral range	Altitude range
HDO	4H2O0008	1420.325–1423.325 cm^{-1}	6–68 km
	4H2O0009	1225.600–1228.000 cm^{-1}	6–33 km
	4H2O0010	1468.925–1471.925 cm^{-1}	6–52 km
	4H2O0011	1486.275–1489.275 cm^{-1}	6–47 km
	4H2O0012	1433.425–1436.425 cm^{-1}	6–33 km
	4H2O0013	1370.225–1373.225 cm^{-1}	6–30 km
	4H2O0014	1429.275–1432.275 cm^{-1}	6–68 km

3 Results

Three to four days per month (approximately evenly spaced) were processed between July 2002 and March 2004. The data presented in this paper is the result of sixty-four days in total. There are around 14 Envisat orbits per day and around 72 limb profile scans per orbit, resulting in approximately 1000 profiles per day. Some post–processing was applied in the calculation of averages. Points where the sum of the row of the averaging kernels were less than some value (arbitrarily set to 0.8) were neglected.

3.1 Zonal mean distribution of HDO

Figure 3 shows seasonal zonal means of δD–HDO. Seasonal zonal means of H_2O are shown alongside for the purposes of comparison. Recall that the results shown here have been retrieved from cloud–free spectra. The seasonal zonal means are therefore biased towards cloud–free cases. It is not presently known how the ability to include cloudy conditions would affect the seasonal zonal means shown here, although it is almost certainly an issue below the tropopause. Given the likely difference in isotopic composition associated with convection versus slower ascent, the bias is likely non–trivial. Stratospheric points (at least in non–polar regions) should not be affected by cloud, but particularly cold or dry data in the stratosphere may not pass the averaging kernel quality check, due to low sensitivity in the spectra to HDO under these conditions. Therefore the stratospheric data, particularly in the tropical lower stratosphere, is likely to be biased towards warmer, more moist and less depeleted conditions and therefore might be expected to show a positive bias in the δD values in this region.

The maximum depletions in the seasonal zonal mean fields are observed in the region of the tropical tropopause, with magnitudes of around -700 ‰. The MIPAS values are well within the range of -460 to -870 ‰ observed by Webster and Heymsfield (2003) in this region. The altitude of the area of maximum depletion is below the altitude of the minimum water vapour values. This is consistent with results from aircraft data in the region of convection near Costa Rica (Gettelman and Webster 2005) and with results of simulations using the GISS model (Schmidt *et al.* 2005). Schmidt *et al.* (2005) note that the minimum isotope ratio near the tropical tropopause is not the same as the "entry value" into the stratosphere. The MIPAS results shown here support this by showing maximum depletions lower than values of entry into the stratosphere typically quoted. The MIPAS "entry values" of δD to the stratosphere vary according to season, but are of the order of -620 to -650 ‰, in good agreement with values of -648 ‰ and -635 ‰ quoted by Kuang *et al.* (2003) and McCarthy *et al.* (2004) respectively. The maximum depletions in the tropopause region correspond to the time of year (March–May) where the minimum temperatures at the tropical tropopause occur. Above the tropopause, there is a general increase in δD with altitude, due to the formation of HDO by the oxidation of CH_3D.

The fields of δD also show a local maximum in the tropical zonal mean profiles at around 50–70 mbar (around 450 K, 18–21 km). This feature is most pronounced in the months of March to May, when the temperatures in this region are at their lowest. We believe that this feature is related to the spatial sampling of the measurements after the cloud and averaging kernel based quality checks have been applied to the retrievals. The coverage of measurements that pass the quality checks is very sparse over convectively active regions such as the tropical Western Pacific, central Africa and central South America. Reasons for this include cloud cover, low temperature and low water vapour, all of which lead to reduced sensitivity to HDO lines in the MIPAS spectra. The sensitivity of the retrieval is generally somewhat higher at, say, 20 mbar than at, say, 70 mbar due to higher H_2O mixing ratios.

In addition to the tropical tropopause region, strong depletions can also be seen in Figure 3 in the southern polar lower stratosphere. This region shows strong depletion for all seasons, but the depletion is strongest in winter, suggesting that it is probably related to polar stratospheric clouds and associated dehydration of the

DOI: 10.1002/qj

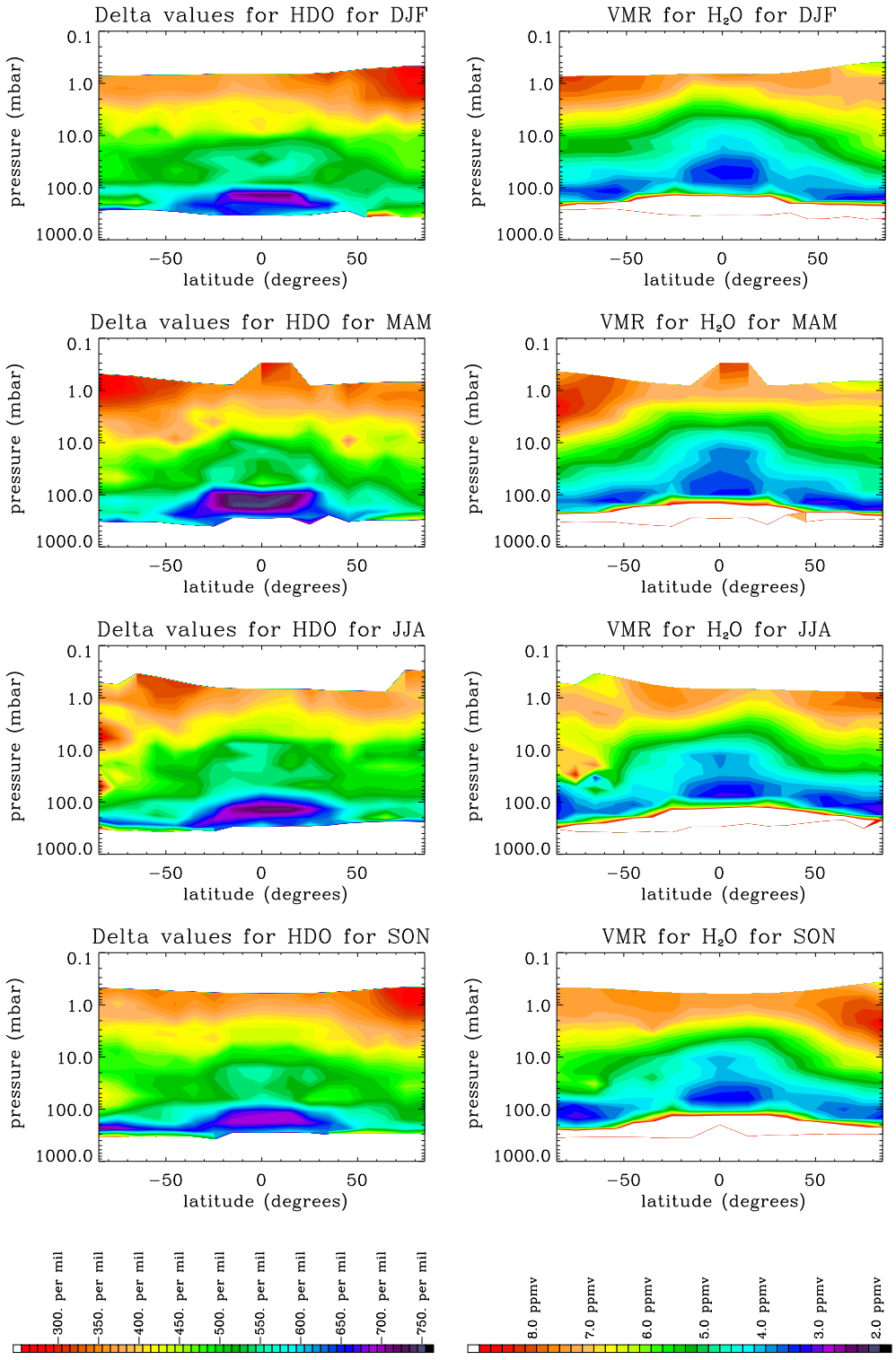

Figure 3. Seasonal zonal mean fields of δD–HDO (left column) and H_2O (right column) from MIPAS measurements.

polar stratosphere (Stowasser *et al.* 1999). A strong vertical oscillation can be seen in the δD southern polar winter. This is believed to be a retrieval artifact, stemming from low sensitivity due to cold temperatures and low water vapour amounts in the polar vortex in this season.

3.2 Comparisons with ATMOS measurements

In order to put the MIPAS measurements into context, Figure 4 shows zonal mean profiles from this MIPAS dataset alongside mean profiles from ATMOS space shuttle measurements in three latitude regions. The mid-latitude comparison shows a MIPAS seasonal zonal

DOI: 10.1002/qj

mean profile from months from March to May in 2003, 40°-50°S, alongside an ATMOS zonal mean from April 29th to May 1st 1985, 47°S (Rinsland *et al.* 1991). The sub-tropical comparison shows a MIPAS seasonal zonal mean from March to May 2003, 20°-30°S, alongside an ATMOS zonal mean from April 29th to May 1st 1985. The tropical comparison shows MIPAS zonal mean profiles for November 2002/2003, 10°-10°S, with ATMOS profiles from 11th and 12th November 1994 (Kuang *et al.* 2003). Profiles are not matched in time or geographical location, and so might be expected to show differences. The tropical profiles show good agreement in the region of maximum depeletion, but ATMOS profiles are around 100 ‰ more depleted than MIPAS profiles in the stratosphere. Large differences could exist if the dates of the ATMOS profiles coincided with a period of particularly strong ascent. MIPAS profiles are around 50 ‰ less depleted than the mid–latitude ATMOS profiles in the stratosphere. However,the vertical variation of the profiles in the stratosphere is similar for the latitude ranges shown, indicating that the two sets of measurements capture the same seasonal and geographical variations.

3.3 Tropical mean profiles

Figure 5a shows the decrease in methane concentration with elevation due to oxidation. Air in the descending branch of the Brewer-Dobson circulation (higher latitudes) is characterized by lower CH_4 values. Isentropic mixing at lower elevations brings the concentration of methane in the region of the tropopause and lower stratosphere towards a more uniform mixing ratio of around 1.7 ppmv. A similar situation can be see in Figure 5b in the isotopic composition of water vapor. In mid–latitudes, profiles of δD from the MIPAS measurements show a decrease in depletion with altitude in the stratosphere, due to the production of HDO by oxidation of CH_3D, which is less depleted in deuterium than water vapour originating from the troposphere. The profiles are plotted using potential temperature as a vertical co-ordinate in order to more readily compare the situation for different latitudes. (Potential temperature values were calculated from MIPAS retrieved pressures and temperatures.)

The total number of hydrogen atoms ("total hydrogen"), is defined approximately as $H_{total} = H_2O + 2 \times CH_4 + H_2$ and is conserved in the stratosphere. "Total deuterium", $D_{total} = HDO + CH_3D + HD$, similarly reflects the approximate conservation of deuterium atoms. Multiply–deuterated species and other minor deuterium-containing species are assumed to be negligible. Using high precision measurements of CH_4, CH_3D, H_2 and HD and using HDO measurements from the FIRS-2 instrument (HDO measurements described in Johnson *et al.* (2001a)), McCarthy *et al.* (2004) report a value for the total deuterium content of 1.60 $(+0.02/-0.03)$ ppbv. McCarthy *et al.* were also able to deduce linear relationships between mixing ratios of CH_4, CH_3D and HD based on their lower stratospheric aircraft measurements (in ppbv):

$$CH_3D = 5.16 \times 10^{-4} + 0.0908 \quad (3)$$

$$HD = -6.32 \times 10^{-5} + CH_4 + 0.297 \quad (4)$$

McCarthy *et al.*'s "total deuterium" value can then be used to calculate what the HDO mixing ratio should be for a given CH_4 mixing ratio. Knowing the total deuterium and hydrogen at the tropopause, and applying equations 3 and 4, a theoretical HDO profile that accounts only for oxidation chemistry has been obtained. This theoretical profile is shown as a dotted line in Figure 5b. The gradient of this profile shows the increase in δD with altitude that would be expected to occur due to the production of HDO from the oxidation of CH_3D and HD in the stratosphere. It can be seen that at higher altitudes the profiles from all latitudes tend towards a gradient which is consistent with the theoretical line, showing that the oxidation source dominates in the stratosphere.

Free from seasonal variation, it might be expected that the averaged profiles would show a minimum just below the tropopause, and then follow this theoretical gradient from thereon upwards. Given that this idealised oxidation curve must fit the upper stratospheric profile, we can extrapolate back to the minimum value. Broadly speaking, this does appear to be the case in mid–latitudes. In the tropics, however, the shape of the profiles is different. The profiles do show a strong minimum just below the TTL, but there is a much sharper gradient between the base of the TTL and the lower stratosphere than can be accounted for by methane oxidation.

Figure 5c shows the correlation between zonal means of δD and CH_4 for stratospheric points in the different latitude bands. The separation between the high latitude and tropical curves at around 1 ppmv of CH_4 illustrates the importance of the interplay between chemistry and dynamics. The curves are separated by around 50 ‰, somewhat larger than the estimated error of 20 ‰ on the δD values. These results show quantitatively that the enrichment of high-latitude upper stratospheric water vapour relative to the tropics of around 80 ‰ is due to methane oxidation. In the mid–stratosphere, the higher latitude water vapor is less depleted (it has a longer history of oxidation). In the tropical lower stratosphere, evidence of strong isentropc mixing between the tropics and higher latitudes is seen in both the methane and the δD.

3.4 Distribution of values

Given the motivating discussion of entry and dehydration mechanisms, it is clear that by examining only the mean distribution, the underlying processes that control conditions in the TTL and stratospheric humidity are easily masked. The characteristics of probability distributions

DOI: 10.1002/qj

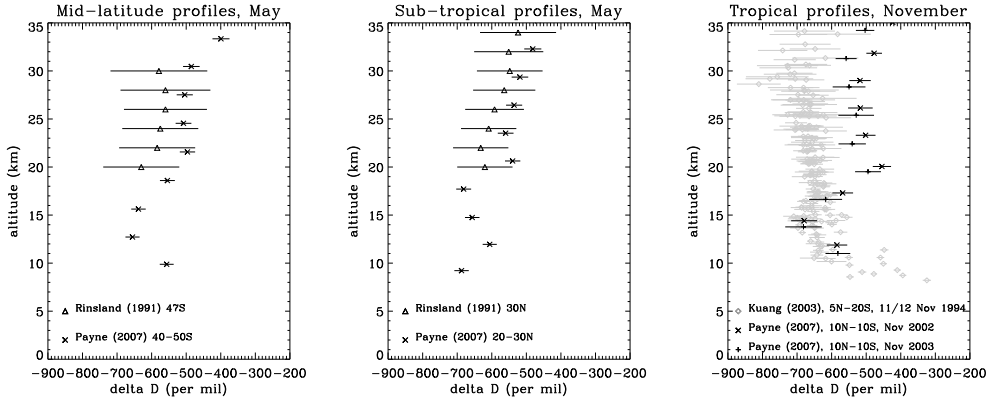

Figure 4. Comparisons of MIPAS and ATMOS profiles of δD. The mid-latitude comparison shows a MIPAS seasonal zonal mean profile from months from March to May in 2003, 40°-50°S, alongside an ATMOS zonal mean from April 29th to May 1st 1985, 47°S (Rinsland *et al.* 1991). The sub-tropical comparison shows a MIPAS seasonal zonal mean from March to May 2003, 20°-30°S, alongside an ATMOS zonal mean from April 29th to May 1st 1985. The tropical comparisons shows MIPAS zonal mean profiles for November 2002/2003, 10°-10°S, with ATMOS profiles from 11th and 12th November 1994 (Kuang *et al.* 2003).

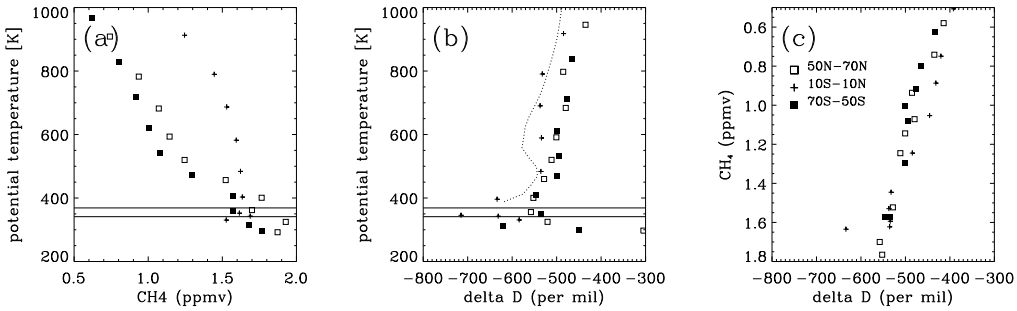

Figure 5. (a) Zonal annual mean profiles of CH_4 from three latitude bands, showing evidence of ascending motion in the tropics and descending motion at higher latitudes. (b) Zonal annual mean profiles of δD from three latitude bands, showing the large depletion in the tropical upper troposphere, the sharp gradient in the TTL and mixing in the stratosphere. The dotted line shows the theoretical gradient profile that would result from formation of stratospheric water vapour from the oxidation of methane and molecular hydrogen. (c) Scatter plot of δD and CH_4 in the stratosphere (points above 380 K). Means for this figure were calculated using all data processed for 2003.

of tracer concentration can allow further insight into transport processes [e.g. Sparling (2000)]. The data were binned according to potential temperature layers (defi ned in Table II). It is worth noting that due to the vertical range of the MIPAS instrument the layer labelled 'Troposphere' will not contain points much below the 6 km instrument viewing range. Probability distributions for δD in these layers for latitudes between $\pm 30°$) are shown in Figure 6. The primary layer of interest here is the TTL where the mixing processes of central importance occur.

An important feature of Figure 6 is that the tropical distributions are skewed towards less depleted values at all levels. This skew in the data suggests that temporal variability is central to the entry processes and that use of a "mean entry ratio", as referred to in the literature (e.g. Moyer *et al.* (1996); Johnson *et al.* (2001b)) is not necessarily the most useful diagnostic. The mean and most probable values of δD in each of the potential temperature layers are shown in Table II. The positive skew in the distributions means that the mean values are typically 100 ‰ less negative than the most probable values.

The δD values were further binned according to their associated water vapour volume mixing ratio (VMR). Since water vapour mixing ratios are so much higher in the troposphere, this gives a measure of tropospheric influence. Retrieved ozone values in the TTL were also binned according to H_2O VMR, in an attempt to determine the importance of a stratospheric origin of the water vapour. Figure 7 shows scatter plots of δD (left column) and O_3 (right column) marked with this additional binning of the data. Also shown in Figure 7, for purposes of comparison, are mid–latitude scatter plots for the same potential temperature layer. In the interpretation of the ozone data in conjunction with water vapour, it is important to note that ozone distributions in the upper troposphere/lower stratosphere are controlled mainly by large–scale advection (horizontal motions) rather than convective processes, while water vapour is influenced strongly by convection (Gettelman *et al.*, 2004). Since each point in the data here represents a simultaneous measurement of H_2O, HDO and O_3, the

DOI: 10.1002/qj

Table II. Atmospheric layers used for calculation of probability distributions

Atmospheric layer	Potential temperature boundaries	Mean δD (‰)	Most probable δD (‰)
Troposphere	less than 340K	−630	−720
Tropopause layer	340–380K	−668	−750
Lower stratosphere	380–500K	−533	−645
Mid–stratosphere	500–700K	−530	−625
Upper stratosphere	greater than 700K	−445	−550

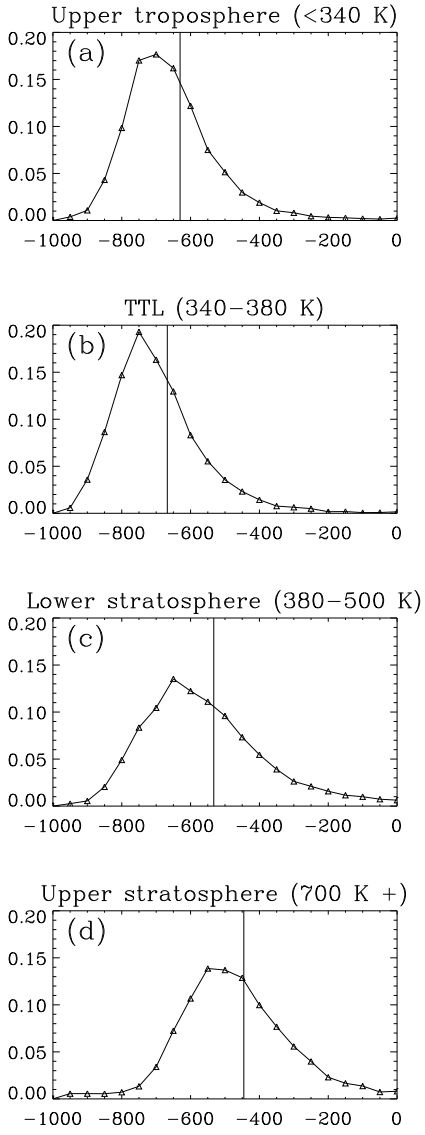

Figure 6. Distributions of values of δD in different atmospheric layers for the tropics and sub-tropics (30°S–30°N); (a) upper troposphere, (b) TTL, (c) lower stratosphere and (d) upper stratosphere. Vertical lines denote the mean value of δD for each layer.

source of depletion can be linked to isentropic mixing of stratospheric air into the TTL.

For H_2O bins between 0 and 10.0 ppmv, the distribution of δD shifts towards more depleted values with increasing H_2O content of the air. TTL air with water vapour mixing ratios between 3 and 10 ppmv shows a gradual shift towards more depleted δD values and a stronger contribution from upward transport from the troposphere (less ozone). The driest air (0–3 ppmv H_2O) exhibits relatively enriched values of δD. While the most common value lies at around −850 ‰, the scatter in δD for the dry points is large. There are a number of dry points showing values δD that are strongly enriched relative to the mean value. These points could be the result of mixing of stratospheric air into the TTL or of the influence of convectively lofted ice. Since ozone values for these driest points do not appear to show a strong stratospheric inluence, we suggest that these anomalously dry points are associated with convective activity (ice lofting) rather than stratospheric mixing into the TTL. From the scatter in the data, it is clear that there are also other mechanisms active. Recall that the random error on individual retrieved points is of the order of 100 ‰, which also explains some part of the scatter.

The activity of the tropics and sub–trpoics is highlighted as the key source region of stratospheric water vapour through contrast with mid-latitude scatter plots at the same potential temperature level (Figure 7). The figure shows distributions of δD which are relatively well–mixed and show little significant dependence on water vapour mixing ratio. Ozone distributions in this potential temperature layer at mid–latitudes appear to be well–mixed. The prevalence of mixing allows the isotopic composition to remain largely unchanged.

The dry, relatively enriched points observed in the tropical/sub-tropical scatter plots in Figure 7 were found to be located mostly in the sub–tropics. The investigation of these points in more detail would be an interesting subject for future work.

3.5 Time series

The temporal variation of δD has the potential to give insight into mechanisms of water vapor transport, since the seasonal timing of the different contributing processes differs. Figure 8 shows time series of H_2O and δD. It is difficult to draw strong conclusions on seasonal cycles based on a 21 month dataset. Tentatively, it appears that δD values in the TTL exhibit an annual cycle, with the most depleted values coinciding with the time of

DOI: 10.1002/qj

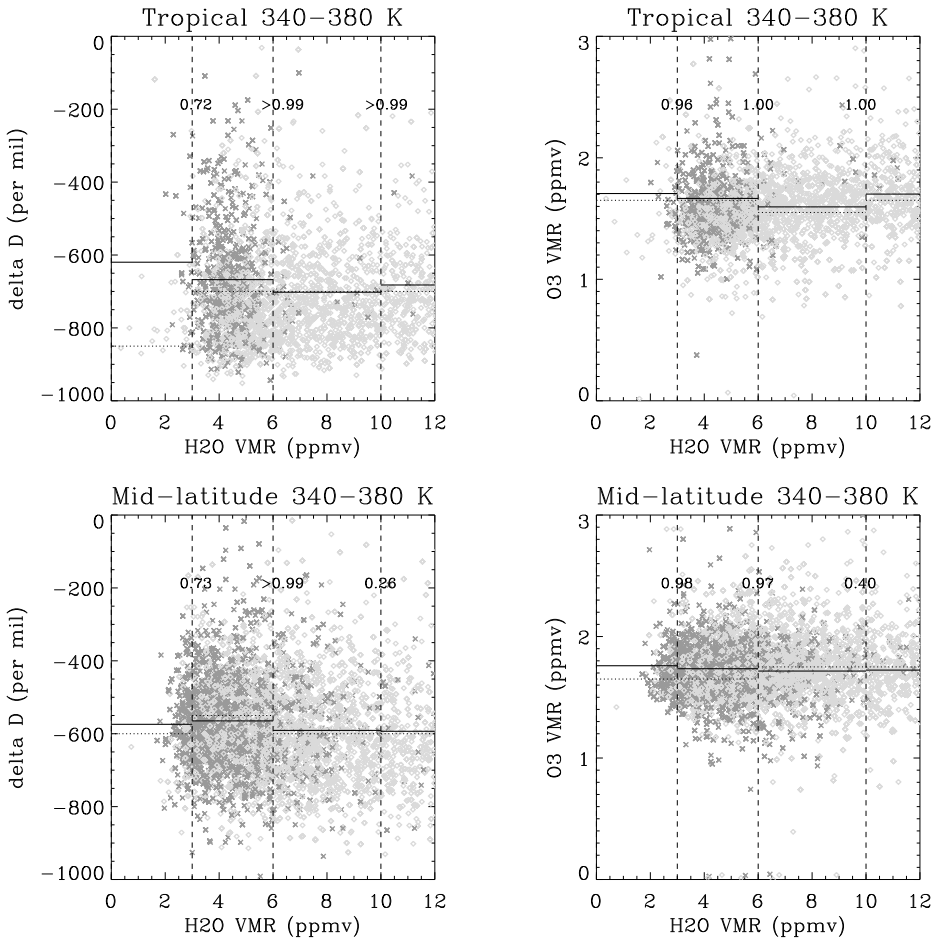

Figure 7. Scatter plots showing δD (left) and O_3 (right) as a function of water vapor in the TTL (340-380 K) and in the same potential temperature layer at mid–latitudes. Lighter diamonds show points with potential temperatures in the range 340-360 K (the lower altitudes range of the layer), while darker crosses show points with potential temperatures in the range 360-380 K (the upper part of the layer). Solid horizontal lines show mean δD (left) and O_3 (right) values in selected H_2O bins, denoted by vertical dashed lines. Numbers associated with these dashed vertical lines show the confidence levels (to two decimal places, from a t–test) that the means in adjacent bins are statistically different. A value of 1.00 means that the confidence level is greater than 99 %. Dotted horizontal lines show the median value in each of the H_2O bins.

year when the tropopause is coldest (May/June). If the tropopause temperature were the main controlling factor for the isotopic composition of water vapour in the stratosphere, the stratospheric time series of mean δD would follow the TTL time series with some time lag, exhibiting the "tropical tape recorder effect" observed in stratospheric water vapour (Mote *et al.*, 1996). Figure 8 suggests that the localized depletions seen at around 10–20 mbar are related to the transport of dry, depleted air upward. However, it appears that sampling biases due to low sensitivity of the retrievals in the tropical lower stratosphere do not allow us to see the tape recorder signal in the δD in the intermediate stages of upward transport. Other factors which could affect the observed variations in depletions in the lower stratosphere include seasonal extrema in convective location/strength and variations in advective transport, convective transport and mixing. Further investigation of seasonal variations in δD would ideally involve a longer dataset. The issue of sampling could perhaps be explored using a global model.

4 Conclusions

This paper presents retrievals of δD in the upper troposphere and stratosphere from space which show unprecedented spatial and temporal coverage. Zonal means show maximum depletions in δD of around -700 ‰ in the tropical upper troposphere. The region of maximum depletion in the tropics is situated at around 200 mbar, well below the altitude of the minimum in the water vapour profile. This is broadly consistent with predictions from models (Schmidt *et al.* 2005). Seasonal zonal means also show an area of maximum depletion in the Southern Hemisphere polar springtime, with values of δD around -750 ‰. This is assumed to be associated with the influence of polar stratospheric clouds and dehydration events in the polar vortex (Stowasser *et al.* 1999). In general, the altitude dependence of δD in the

DOI: 10.1002/qj

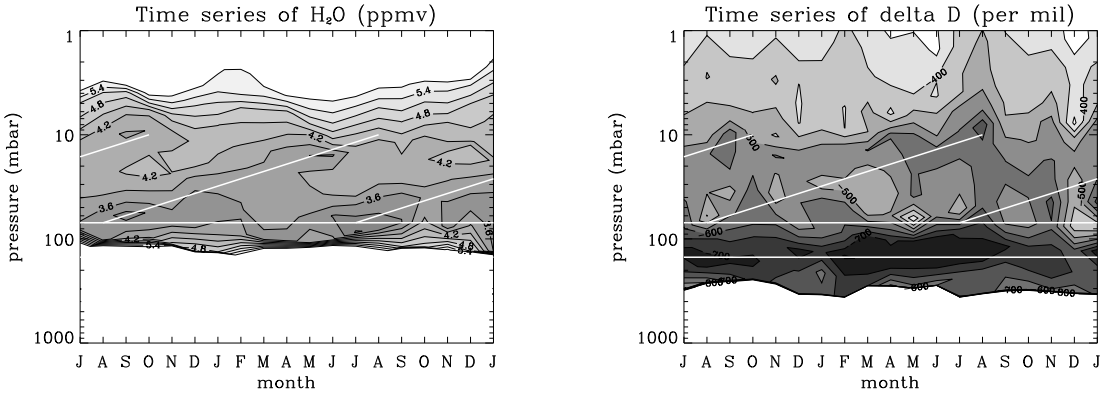

Figure 8. Time series of mean H_2O and δD in the tropics. Horizontal lines denote the approximate boundaries of the TTL at 150 and 70 mbar. Sloping lines on both plots represent the ascent of dry air upwards (the 'tropical tape recorder effect'). Contour intervals are 0.3 ppmv for H_2O and 50 ‰for δD.

stratosphere is consistent with the contribution to the deuterium content of water vapour from oxidation of methane (and molecular hydrogen) (McCarthy *et al.* 2004).

In published studies relating to remotely–sensed measurements of δD, there has been some focus on the concept of a "mean isotopic entry ratio". With the spatial and temporal coverage offered by MIPAS, it is possible to look further than some mean entry ratio. The skewed shape of the probability distributions presented here suggest that, in the tropics, the mean value of δD may not be the most useful quantity to examine when considering the characteristics of entry of water vapour into the stratosphere.

Further analysis of these distributions in terms of water vapour content and of distributions of ozone volume mixing ratios leads to a number of conclusions. A number of the driest observations in the TTL are associated with small depletions (relative enrichment) in δD, due to the influence of ice–lofting associated with rapid convection, and thus not well explained by a Rayleigh paradigm. Moister TTL air shows greater depletion in δD, associated with gradual slow ascent of air and water vapour into the TTL. The very wettest air in the TTL is associated with less depleted δD values again. From the mean ozone values associated with these points, it appears that this very wet air is also associated with stratospheric influence, presumably stemming from downwelling surrounding the areas where the strongest convection overshoots. This is consistent with the stratospheric "drain" described by Sherwood (2000).

The time series of mean δD values in the TTL appear to show evidence of an annual cycle that follows the variation of the temperature at the tropical tropopause. Strong depletions in the mid–stratosphere do appear to be associated with upward transport of this signal. However, the signal cannot be tracked through the lower stratosphere. We believe this is due to a sampling bias, caused by low retrieval sensitivity in the tropical lower stratosphere. In future processing of the MIPAS data, this situation could perhaps be improved by the use of more microwindows in the retrieval to yield higher signal to noise, or by the selection of microwindows targeted specifically at this region.

The MIPAS instrument is unable to provide spatial resolution on the scale of convective events. Nor is MIPAS able to offer sufficient accuracy to make definitive statements on the precise details of the mechanisms outlined here. MIPAS is also limited by its inability to measure in cloudy conditions, in which many of the processes of interest are active. These are challenges which can be addressed by *in situ* measurements or indeed act as design criteria for future satellite missions. The MIPAS data presented here result from processing of only a subset of the available spectra. Further processing of higher data volumes would allow averaging on smaller temporal and spatial scales, and therefore a more extensive investigation of temporal and spatial variation in the isotopic composition of water vapour in the upper troposphere and stratosphere. However, the data presented here does raise some previously unrecognised points. It is clear that the satellite data alone is not enough to interpret and identify individual processes. The satellite data, which includes measurement error, sampling bias and other uncertainty, should be used with some kind of model. In combining the observations with a model, robust interpretations could be made. There are many processes, and we only have observations of a limited number of quantities at limited temporal and spatial resolution. A combination of remotely sensed data, *in situ* data and appropriate process models are needed in combination to fully explain the TTL budget.

DOI: 10.1002/qj

In addition, the MIPAS spectra offer the potential to retrieve profiles of $H_2^{18}O$ and $H_2^{17}O$, which will offer additional useful information, since the signature of individual processes on the triplet of water vapour isotopologues is more unique than that on a single species. Used in conjunction with *in situ* data and models, the MIPAS data offer great potential for future work by allowing integrated understanding of climatologically important hydrologic processes acting on many scales to be developed.

Acknowledgements

The authors would like to thank the Royal Meteorological Society and the Rupert Ford Fund, for supporting the visit made by Vivienne Payne to the University of Colorado in order to facilitate this work. We would also like to thank John Worden and Kevin Bowman at the Jet Propulsion Laboratory in Pasedena as well as Darin Toohey at the Univeristy of Colorado for their helpful input and suggestions and Zhimming Kuang for supplying tropical ATMOS profiles of δD. MORSE was developed under the NERC EO Enabling Fund. We would also like to thank the two anonymous reviwers for their insightful and constructive comments.

References

Boone, C. D. *et al.* 2005 'Retrievals for the atmospheric chemistry experiment Fourier transfrom spectrometer'. *Appl. Opt.*, **44,** 7218–7231

Brewer, A. W. 1949 'Evidence for a world circulation provided by the measurements of helium and water vapour distribution in the stratosphere'. *Q. J. R. Meteorol. Soc.*, **75,** 351–363

Carli, B. et al. 2004 'First results of MIPAS/ENVISAT with operational Level 2 code'. *Advances in Space Research*, **33 (7),** 1012–1019

Coffey, M. T, Hannigan, J. W. and Goldman, A. 2006 'Observations of upper tropospheric/lower stratospheric water vapor and its isotopes'. *J. Geophys. Res.*, **111,** D14313, doi:10.1029/2005JD006093

Danielson, E. F. 1982 'A dehydration mechanism for the stratosphere'. *Geophys. Res. Lett.*, **9,** 605–608

Dansgaard, W. 1964 'Stable isotopes in precipitation'. *Tellus*, **16,** 436-468

Dinelli, B. M., Carli, B. and Carlotti, M. 1991 'Measurement of stratospheric distributions of $H_2^{16}O$, $H_2^{18}O$, $H_2^{17}O$ and $HD^{16}O$ from far IR spectra'. *J. Geophys. Res.*, **96,** 7509–7514

Dudhia, A., Jay, V. L. and Rodgers, C. 2002a 'Microwindow selection for high spectral resolution sounders'. *Appl. Opt.*, **41,** 3665–3673

Dudhia, A., Morris, P. E. and Wells, R. J. 2002b 'Fast monochromatic radiative transfer calculations for limb sounding'. *J. Quant. Spec. and Rad. Trans.*, **74,** 745–746

Dudhia, A 2005 'MORSE: MIPAS Orbital Retrieval using Sequential Estimation'. *http://www.atm.ox.ac.uk/MORSE*

Enhalt, D.H. 1974 'Vertical profiles of HTO, HDO and H_2O in the troposphere'. *Tech Note TN/STR100, NCAR*, **7,** 307-313

ESA 2000 'Envisat MIPAS —an instrument for atmospheric chemistry and climate research'. Technical Report, European Space Agency, ESA/SP–1229

Fischer, H. and Oelhaf, H. 1996 'Remote sensing of vertical profiles of atmospheric trace constituents with MIPAS limb–emission spectrometers'. *Appl. Opt.*, **35,** 2787–2796

Forster, P. M. D. and Shine, K. P. 1999 'Stratospheric water vapour changes as a possible contributor to observed stratospheric cooling'. *Geophys. Res. Lett.*, **26,** 3309–3312

Fristsch. J. and Brown, J 1982 'On the generation of convectively driven mesohighs aloft'. *Mon. Weather. Rev.*, **101,** 1554–1563

Gettelman, A. *et al.* 2004 'Impact of monsoon circulations on the upper troposphere and lower stratosphere'. *J. Geophys. Res.*, **109,** D22101

Gettelman, A. and Webster, C. R. 2005 'Simulations of water isotope abundances in the upper troposphere amd lower stratosphere and implications for stratosphere troposphere exchange'. *J. Geophys. Res.*, **110,** D17301

Holton, J. R. and Gettelman, A. 2001 'Horizontal transport and the dehydration of the stratosphere'. *Geophys. Res. Lett.*, **28,** 2799-2802

Johnson, D. G. *et al.* 2001a 'Isotopic composition of stratospheric water vapor: Measurements and photochemistry'. *J. Geophys. Res.*, **106,** 12211–12218

Johnson, D. G. *et al.* 2001b 'Isotopic composition of stratospheric water vapor:Implications for transport'. *J. Geophys. Res.*, **106,** 12219–12226

Kirk–Davidoff, D. B. *et al.* 1999 'The effect of climate change on ozone depletion through changes in stratospheric water vapour'. *Nature*, **402,** 399–401

Kuang, Z. *et al.* 2003 'Measured HDO/H_2O ratios across the tropical tropopause'. *Geophys. Res. Lett.*, **30,** 1327, 10.1029/2003GL017023

McCarthy, M. C. *et al.* 2004 'The hydrogen isotopic composition of water vapor entering the stratosphre inferred from high–precision measurements of δD–CH_4 and δD–H_2'. *J. Geophys. Res.*, **109,** d07304, 10.1029/2003JD004003

Mote, P. W. *et al.* 1996 'An atmospheric tape recorder: the imprint of tropical tropopause temperatures on stratospheric water vapor'. *J. Geophys. Res.*, **101,** 3989–4006

Moyer, E. J. *et al.* 1996 'ATMOS stratospheric deuterated water and implications for troposphere–stratosphere transport'. *Geophys. Res. Lett.*, **23,** 2385–2388

Mulvaney, R. and Wolff, E. W. 1993 'Evidence for winter spring denitrification of the stratosphere in the nitrate record of Antarctiv fern cores'. *J. Geophys. Res.*, **98 (D3),** 5213–5220

Nordh, H.L. *et al.* 2003 'The Odin orbital observatory'. *Astronomy and Astrophysics*, **402,** 21–25

Payne, V. H. 2005 'Retrievals of water vapour and methane from the MIPAS satellite instrument'. PhD thesis, University of Oxford

Potter, B. E. and Holton, J. R. 1995 'The role of monsoon convection in the dehydration of the lower tropical stratosphere'. *J. Atmos. Sci.*, **52,** 1034–1050

Ridofi, M. et al 2000 'Optimised forward model and retrieval scheme for MIPAS near–real–time data processing'. *Applied Optics*, **39,** 1323-1340

Robinson, G. D. 1980 'The transport of minor atmospheric constituents between troposphere and stratosphere'. *Q. J. R. Meteorol. Soc.*, **106,** 227–253

Rodgers, C. D. 2000 *Inverse methods for atmospheric sounding: Theory and Practice.* World Scientific

Rosenlof, K. H. 2001 'Stratospheric water vapor increases over the past half–century'. *Geophys. Res. Lett.*, **27,**, 1195–1198

Rosenlof, K. H. 2003 'How water enters the stratosphere'. *Science*, **302,** 1691–1692

Rozanski, K. and Sonntag, C. 1982 'Vertical distribution of deuterium in atmospheric water vapour'. *Tellus*, **34,** 134–141

Salawitch, R. J. *et al.* 1989 'Denitrification in the Antarctic stratosphere'. *Nature*, **339,** 525–527

Schmidt, G. A. *et al.* 2005 'Modelling atmospheric stable water isotopes and the potential for constraining cloud processes and stratosphere–troposphere water exchange'. *J. Geophys. Res.*, **110,** D21314

Sherwood, S. C. 2000 'A stratospheric "drain" over the maritime continent'. *Geophys. Res. Lett.*, **27,** 677–680

Sherwood, S. C. and Dessler, A. E. 2000 'On the control of stratospheric humidity'. *Geophys. Res. Lett.*, **27,** 2513–2516

Smith, R. B. 1992 'Deuterium in North Atlantic storm tops'. *J. Atmos. Sci.*, **49,** 2041–2057

Spang, R., Remedios, J. and Barkley, M. 2004 'Cloud indices for the detection and differentiation of cloud types in infrared limb emission spectra'. *Advances in Space Research*, **33,** 1041–1047

Sparling, L. C. 2000 'Statistical perspectives on stratospheric transport'. *Reviews of Geophysics*, **38,** 417-436

Stowasser, M. et al 1999 'Simultaneous measurements of HDO, H_2O and CH_4 with MIPAS–B: Hydrogen budget inside the polar vortex'. *J. Geophys. Res.*, **104,** 19213-19255

Taylor, C.B. 1972 The vertical variations of isotopic concentrations

DOI: 10.1002/qj

of tropospheric water vapour over continental Europe, and their relationship to tropospheric structure'. *Report INS-R-107, Institute of Nuclear Science, Lower Hutt, New Zealand*

Urban, J. *et al.* 2004 'Odin/SMR observations of stratospheric water vapour and its isotopes: requirements on spectroscopy'. *Proceedings of the International Workshop on Critical Evaluation of mm–/submm–wave Spectroscopic data for Atmospheric Observation*, Ibaraki, Japan

Vömel, H. *et al.* 2002 'Balloon–borne observations of water vapor and ozone in the tropical upper troposphere and lower stratosphere'. *J. Geophys. Res.*, **107,** D144210

Webster, C. R. and Heymsfield, A. J. 2003 'Water isotope ratios D/H, $^{18}O/^{16}O$, $^{17}O/^{16}O$ in and out of clouds map dehydration pathways'. *Science*, **302,** 1742–1745

Winker, D. M. amd Trepte, C. R. 1998 'Laminar cirrus observed near the tropical tropopause by LITE'. *Geophys.Res. Lett.*, **25,** 3351–3354

WMO 2000 'Stratospheric Processes and their Role in Climate (SPARC) assessment of upper tropospheric and stratospheric water vapour'. *SPARC Rep. 2, WRCP-113, WMO/TD-1043*, Geneva

Worden, J. *et al.* 2006 'TES observations of the tropspheric HDO/H_2O ratio: Estimation approach and characterization'. *Accepted to J. Geophys. Res.*

Wu, D. L. *et al.* 2006 'EOS MLS cloud ice measurements and cloudy–sky radiative transfer model'. *IEEE TGRS*, **44,** 1156-1165

Zahn, A. *et al.* 1998 'Deuterium, tritium and oxygen–18 as tracers for water vapour transport in the lower stratosphere and tropopause region'. *J. Atmos. Chem.*, **30,** 25–47

DOI: 10.1002/qj